

Formation kinetics of crystalline $\text{Ti}_{1-x}\text{Cr}_x\text{O}_2$ photocatalyst from its amorphous powder

E. D. Jeong^a, S. M. Yu^a, J. H. Yoon^a, J. S. Bae^a, T. E. Hong^a, C. R. Cho^b, K. T. Lim^c, P. H. Borse^{d,*} and H. G. Kim^{a,*}

^aBusan Center, Korea Basic Science Institute, Busan 609-735, Korea.

^bDepartment of Nano Fusion Technology, Pusan National University, Pusan 609-735, Korea

^cDepartment of Imaging System Engineering, Pukyong National University, Busan 609-735, Korea.

^dSolar H_2 PEC lab, International Advanced Research Centre for Powder Metallurgy and New Materials (ARC International), Balapur PO, Hyderabad, AP, 500 005, India.

Amorphous powders of undoped and chromium-doped TiO_2 were prepared by a sol-gel method. Corresponding crystalline (anatase/rutile) phases were obtained by thermally-induced transformation of these amorphous powders. The activation energies for crystallization and grain growth of crystalline TiO_2 and $\text{Ti}_{0.9}\text{Cr}_{0.1}\text{O}_2$ from respective amorphous counterparts were estimated from X-ray diffraction and differential thermal analysis studies. The activation energies required for grain growth in amorphous TiO_2 and $\text{Ti}_{0.9}\text{Cr}_{0.1}\text{O}_2$ samples, were 1.51 kJ/mol and 1.78 kJ/mol, respectively. The activation energies required for the phase transformation from amorphous to crystalline TiO_2 and $\text{Ti}_{0.9}\text{Cr}_{0.1}\text{O}_2$ were 132 kJ/mol and 153 kJ/mol, respectively. It has been clearly demonstrated that relatively a higher temperature is required for the phase transformation in amorphous Cr doped TiO_2 than in amorphous TiO_2 . This can be attributed to the high energy required for the substitution of Cr at Ti site in the TiO_2 lattice, which in turn also yields a smaller crystallite size during grain growth.

Key words: TiO_2 , Activation energy, Cr-doped TiO_2 , Sol-Gel method.

Introduction

Solar energy can be photocatalytically converted into clean hydrogen energy by splitting water. It can also be utilized to photocatalytically decompose toxic organic or inorganic pollutants to purify water and air, and to provide superhydrophilicity to solid surfaces [1-5]. Several applications are known to focus on economic TiO_2 , which shows tremendous activity and long-term stability [6]. Nevertheless, TiO_2 is active only under ultraviolet (UV) light (wavelength < 400 nm) due to its wide band-gap energy of *ca.* 3.2 eV (for the anatase crystalline phase). Since, the fraction of UV in the solar spectrum is less than 5%, TiO_2 photocatalysis cannot efficiently exploit the abundant natural resource *i.e.* solar radiation which dominantly consists of visible light. In order to utilize the main part of the solar spectrum, for outdoor and even for indoor applications under weak interior lighting, photocatalysts absorbing visible light are required. Hence, development of visible-light active photocatalytic materials is a subject of extensive current research in this field.

One of the promising approaches to develop new photocatalysts is the tuning of the optical properties of

UV light active catalysts by substitutional doping, as demonstrated in TaON [7], $\text{TiO}_{2-x}\text{C}_x$ [8], or $\text{TiO}_{2-x}\text{N}_x$ [9] for anion doping. Although, this substitutional doping, in most of the cases, resulted in a small absorption in the visible light region with the original band gap absorption intact, rather than a total red-shift of the band gap energy. In addition there is concern for the stability of substituted anions under the reaction conditions. The metal cation-doped TiO_2 particles are still interesting as they absorb visible light photons. Choi et al. [10] reported that the absorption edge of metal-doped TiO_2 shifted to the visible light region. Anpo and coworkers [11-12] showed that ion implantation of V, Cr and several transition metals shifted the absorption edge to the visible light region. Recently, we have also succeeded in fabricating metal-doped TiO_2 [13]. These materials showed stability in reaction systems involving water or air. As reported, it was found that at an optimum Cr concentration enhanced photocatalytic performance was obtained in a $\text{Ti}_{1-x}\text{Cr}_x\text{O}_2$ system photocatalyst. It motivated us to study the kinetic formation of the optimal concentration Cr doped sample TiO_2 in the present study.

Although metal-doped TiO_2 has been widely studied for the photocatalytic decomposition of acetaldehyde to CO_2 under visible light irradiation, however the thermodynamic energy required for substitution of metal for Ti in TiO_2 has not been investigated. In the present study, the formation kinetics and crystallization

*Corresponding author:

Tel : +82-51-974-6104

Fax: +82-51-974-6116

E-mail: phborse@arci.res.in ; hhgkim@kbsi.re.kr

behaviors of $Ti_{1-x}Cr_xO_2$ in amorphous chromium-doped TiO_2 powders prepared by a sol-gel method were investigated using X-ray diffraction (XRD) and differential thermal analysis (DTA) techniques. The activation energies for crystallization and grain growth of $Ti_{1-x}Cr_xO_2$ were obtained from these data and were analyzed to understand the thermo-chemic behavior specifically for the optimum chromium concentration.

Experimental

TiO_2 sol was prepared from a titanium isopropoxide $Ti(OCH(CH_3)_2)_4$ (99.0%, Aldrich Co.) precursor using a controlled sol-gel method. Briefly, 5 ml of 1.0 M solution of $Ti(OCH(CH_3)_2)_4$ prepared in absolute ethanol was added drop-wise under vigorous stirring to 46 ml of distilled water. The mixture pH was adjusted to pH \sim 1.77 using nitric acid. An aqueous solution of 0.1 molar $Cr(NO_3)_3 \cdot 6H_2O$ was prepared and slowly added drop-by-drop to the TiO_2 sol in a water bath with continuous stirring. The stirring was continued for 2 h at 50 until it became a transparent greenish or reddish clear solution for Cr-mixed TiO_2 . Next, the gel was dried at 80 to yield powder. These samples were calcined at 170 for 5 hr in an electric furnace to obtain amorphous powders of TiO_2 .

These treated amorphous powders thus obtained were characterized by powder X-ray diffraction (XRD, Mac Science Co., M18XHF). For each powder, the characteristic temperatures, such as glass transition (T_g) and primary (T_p) exothermic peaks, were determined using differential thermal analysis (DTA: TA Instruments SDT Q600, USA). DTA scans at the heating rates of 10, 20, 30 and 40 $Kmin^{-1}$, were performed on the amorphous powders up to 700 °C.

Results and Discussion

In order to analyze the crystallization behavior of the anatase phase in amorphous TiO_2 powders prepared by the sol-gel method, respective powder XRD patterns were recorded and are shown in Fig. 1 in the 2θ range of 10-70 °. As observed in Fig. 1, no crystalline phase was detected in the precursor sample (a). However, the samples showed a systematic evolution of crystalline phases with a change in the treatment temperature. TiO_2 crystals in amorphous samples grew with increasing calcinations temperatures. The crystallization of anatase crystals in the precursor samples was completed between 300 °C and 450 °C. Application of Scherrer's equation on the half width of XRD peaks gave a crystal size of 15 nm. The observed lattice parameters of anatase TiO_2 with a tetragonal crystal structure was estimated to be $a = b = 3.78 \text{ \AA}$ and $c = 9.49 \text{ \AA}$. It is important to state that the chromium doped amorphous sample behaved in a similar way to undoped sample.

Figure 2 displays a comparison of XRD patterns of

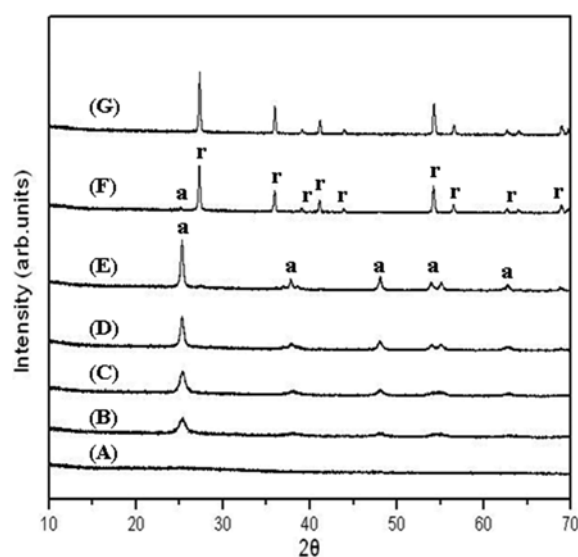


Fig. 1. Powder XRD patterns of (A) TiO_2 precursor sample; and of the crystals formed in these samples after heat-treating at (B) 300 °C, (C) 350 °C, (D) 400 °C, (E) 450 °C, (F) 550 °C and (G) 650 °C. Anatase: (a); Rutile: (r).

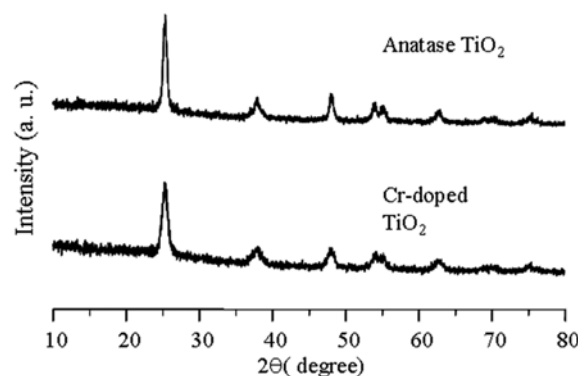


Fig. 2. Powder XRD patterns of undoped and Cr-doped TiO_2 prepared from precursors prepared in the present study, by calcination at 450 °C, 2 h

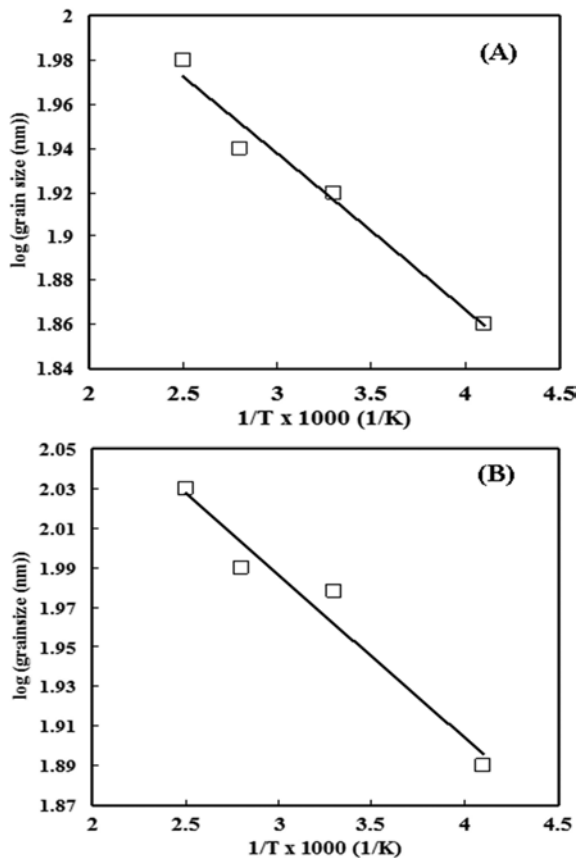
the undoped and Cr doped sample treated at 450 °C for 2 h indicating a similarity in the nature of the patterns. The average size of crystals formed in $Ti_{0.9}Cr_{0.1}O_2$ sample and TiO_2 sample were estimated from the full width at half maxima (FWHM) of XRD peak (Fig. 2) using Scherrer's equation [14]:

$$D = 0.9\lambda/B\cos\theta \quad (1)$$

Here λ is the wavelength of the X-ray radiation ($\lambda = 0.154 \text{ nm}$), B is the FWHM of the peak (in radians) corrected for instrumental broadening, θ is the Bragg angle, and D is the crystallite size (\AA). The crystallite sizes for the chromium doped TiO_2 powder (CTP) sample and amorphous TiO_2 powder (ATP) sample are given in Table 1. Interestingly, it was found that at the same calcination temperature, the crystallite size of TiO_2 formed in the ATP sample is smaller than that of $Ti_{0.9}Cr_{0.1}O_2$ formed from the CTP sample. The $Ti_{0.9}Cr_{0.1}O_2$ crystals in the CTP sample grew more

Table 1. crystallite size (nm) of Cr-doped TiO₂ and TiO₂.

Temperature (°C)	TiO ₂	Cr-doped TiO ₂
	Crystalline size (nm)	Crystalline size (nm)
300	7.81	7.28
350	9.51	8.33
400	9.98	8.89
450	10.73	9.69

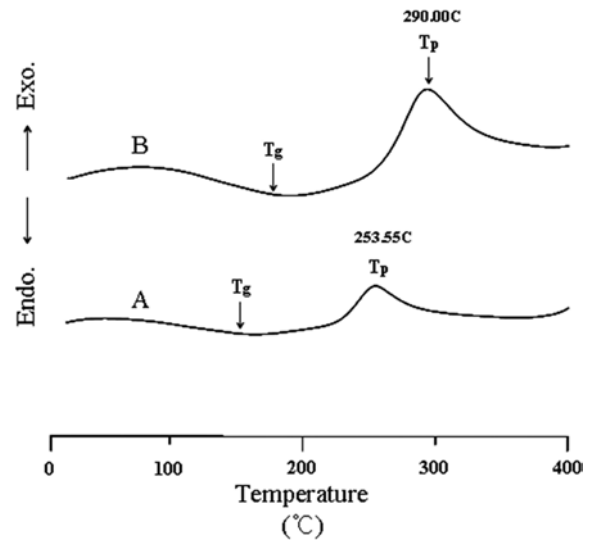
**Fig. 3.** A plot of log of grain size (of TiO₂ in amorphous samples calcined for 2 h at 250 °C, 300 °C, 350 °C, and 400 °C) versus the reciprocal of absolute temperature (1/T) for the (A) ATP and (B) CTP samples.

slowly relative to that of TiO₂ in the ATP sample. The activation energy required for grain growth of Ti_{0.9}Cr_{0.1}O₂ and TiO₂ in respectively in the CTP sample and the ATP sample could be estimated by Arrhenius plots of the crystallite size results. According to Coble's theory [15], the activation energy of grain growth can be calculated by the Arrhenius equation :

$$d \ln k = \frac{E}{RT^2}, \quad (2)$$

where k is the specific reaction rate constant, E is the activation energy, T is the absolute temperature and R is the ideal gas constant.

Jarcho et al. [16] discovered the value of k directly relates with the grain size. Thus modification and

**Fig. 4.** DTA patterns for undoped (A) and Cr Doped (B) TiO₂ precursor systems. The heating rate was 10 Kminute⁻¹.**Table 2.** Endothermic peak temperatures (°C) for various samples.

Scan rate (Kminute ⁻¹)	Amorphous TiO ₂	Amorphous Cr-doped TiO ₂
	Edo. temp. (°C)	Edo. temp. (°C)
10	253.51	290.00
20	256.23	297.26
30	258.87	304.61
40	261.17	311.95

integration of Eq. (2) yields:

$$\log D = (-E/2.303 R)/T + A, \quad (3)$$

where D is the grain size and A is the intercept. From a plot of $\log D$ versus the reciprocal of the absolute temperature ($1/T$) from Eq. (3), one obtains a straight-line as obtained in Fig. 3(A) and (B). The slope of the line gives the activation energies of grain growth of Ti_{0.9}Cr_{0.1}O₂ and TiO₂ crystals in CTP and ATP samples respectively. The activation energies of grain growth of Ti_{0.9}Cr_{0.1}O₂ and TiO₂ were determined to be 1.78 kJ/mol and 1.51 kJ/mol, respectively. Thus, the activation energy required for formation of Ti_{0.9}Cr_{0.1}O₂ crystals in the CTP sample is higher relative to formation of TiO₂ in the ATP sample.

Thermal behavior of both the CTP sample and ATP sample were investigated by differential thermal analysis (DTA). DTA curves of both the ATP and the CTP samples in the temperature range of 50-900 °C with heating rates of 10 Kminute⁻¹ are shown in Fig. 4 (A) and (B), respectively. An exothermic peak, for both the samples was identified in the respective spectrum. In the case of CTP, the appearance of the exothermic peak near 290 °C in the curve corresponds to the transformation from amorphous to anatase

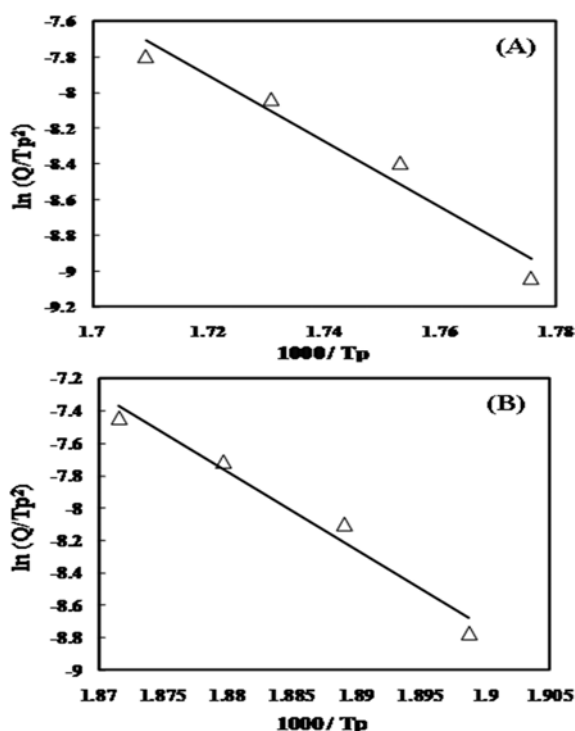


Fig. 5. The plot of $\ln(Q/T_p^2)$ vs. $(1000/T_p)$ to obtain the activation energies involved in the crystallization in the anatase phase transformation in (A) ATP and (B) CTP samples.

phases and the results were in good accordance with the XRD studies.

This section describes the detailed investigations on the kinetic behavior of doped and undoped TiO_2 . Table 2 shows the phase transition temperatures at different heating rates for both the CTP sample and ATP sample as determined by DTA studies. The exothermic peaks shifted to a higher temperature region with an increase in the heating rate.

The energy for crystallization of CTP and ATP in precursor samples could be calculated from the different heating rates and the exothermic peak temperature values in Table 2 using the Kissinger's or Redhead's equations as follows [17-18]:

$$\ln(\Phi/T_p^2) = -E/RT_p + \text{const.} \quad (4)$$

where Φ is the heating rate, T_p is the peak temperature and R is the ideal gas constant. As shown in Fig. 5 (A) and (B), the plots of $\ln(\Phi/T_p^2)$ vs. $(1000/T_p)$ for the samples showed a straight line. The energy required for the phase transformation from the CTP sample to $Ti_{0.9}Cr_{0.1}O_2$ was estimated as 153 kJ/mol from the slope of the straight line in Fig. 5(A). Thus, the energy required for crystallization and substitution of chromium in the CTP sample is one of the important factors to consider for fabricating a $Ti_{0.9}Cr_{0.1}O_2$ photocatalyst with a high photocatalytic activity. In the case of the ATP sample, the energy required for the phase transformation to TiO_2 was calculated to be

132 kJ/mol from the slope of the straight line in Fig. 5 (B). The sole contribution due to the size-dependent phase transformation has already been taken care of by using similar (amorphous) starting samples viz. ATP and CTP. Thus, it has been clearly demonstrated that the activation energy required for $Ti_{0.9}Cr_{0.1}O_2$ crystallization in the CTP sample was higher than that of TiO_2 crystallization in the ATP sample.

Conclusions

Chromium-doped amorphous TiO_2 samples were prepared by a sol-gel method. The activation energies for phase transformation kinetics and grain growth of $Ti_{0.9}Cr_{0.1}O_2$ formed by substitution of Cr in chromium-doped TiO_2 amorphous powders were determined from the results of XRD and DTA. The activation energy required for the phase formation and grain growth of $Ti_{0.9}Cr_{0.1}O_2$ in the CTP sample and of TiO_2 in the ATP sample were determined to be 1.78 kJ/mol and 153 kJ/mol, respectively. In comparison to the TiO_2 crystallization in the ATP sample prepared by the sol-gel method, the phase transformation kinetics of $Ti_{0.9}Cr_{0.1}O_2$ in amorphous chromium-doped TiO_2 shows slower crystallization than that of TiO_2 .

Acknowledgements

The authors acknowledge the support of KBSI grant T30320, Hydrogen Energy R&D Center, Korea. The author (PB) also acknowledges the support of Director ARCI, Hyderabad.

References

1. J.S. Lee, Catal. Surv. Asia 9 (2005) 217-227.
2. A. Kudo, Y. Miseki, Chem. Soc. Rev. 38 (2009) 253-278.
3. K. Maeda, T. Takata, M. Hara, N. Saito, Y. Inoue, H. Kobayashi, K. Domen, J. Am. Chem. Soc. 127 (2005) 8286-8287.
4. H.G. Kim, D.W. Hwang, J.S. Lee, J. Am. Chem. Soc. 126 (2004) 8912-8913.
5. J.S. Jang, S.M. Ji, S.W. Bae, H.C. Son and J.S. Lee, J. Photochem. Photobiol. A: Chem., 188 (2007) 112-119.
6. P.H. Borse, L.S. Kankate, F. Dassenoy, W. Vogel, J. Urban, S.K. Kulkarni, J. Mater. Sci., 13 (2002) 553-559.
7. G. Hitoki, T. Takata, J. Kondo, M. Hara, H. Kobayashi, and K. Domen, Chem. Commun. (2002) 1698-1699.
8. S.U.M. Khan, M. Al-Shahry and W.B. Jr. Ingler, Science 297 (2002) 2243-2245.
9. R. Asahi, T. Ohwaki, K. Aoki, Y. Taga, Science, 293 (2001) 269-271.
10. W. Choi, A. Termin, M.R. Hoffmann, Angew. Chem. Int. Ed. Engl. 33 (1994) 1091-1092.
11. H. Yamashita, Y. Ichihashi, M. Takeuchi, S. Kishiguchi and M. Anpo, Synchrotron Radiat. 6 (1999) 451-452.
12. M. Takeuchi and M. Anpo, Intern. J. Photoenergy 3 (2001) 89-94.
13. S.W. Bae, P.H. Borse, S.J. Hong, J.S. Jang, J.S. Lee, E.D. Jeong, T.E. Hong, J.H. Yoon, J.S. Jin and H.G. Kim, J.

- Korean Phy. Soc. 51 (2007) S22-S26.
14. B.D. Cullity, "Elements of X-ray diffraction," 2nd Edition, Addison-Wesley Publishing Company, Inc., Reading, MA, 1978.
15. R.L. Coble, J. Appl. Phys. 32 (1961) 787-792.
16. M. Jarcho, C.H. Bolen and R.H. Doremus, J. Mater. Sci. 11 (1976) 2027-2035.
17. H.E. Kissinger, J. Res. Natl. Bur: Stand. (US) 57 (1956) 217-221.
18. P.A. Redhead, Vacuum. 12 (1962) 203-211.